



# A macroscopic device described by a Boltzmann-like distribution

## Citation

Tricard, Simon, Claudiu A. Stan, Eugene I. Shakhnovich, and George M. Whitesides. 2013. "A Macroscopic Device Described by a Boltzmann-Like Distribution." *Soft Matter* 9 (17): 4480.

## Published Version

doi:10.1039/c3sm27385g

## Permanent link

<http://nrs.harvard.edu/urn-3:HUL.InstRepos:12388525>

## Terms of Use

This article was downloaded from Harvard University's DASH repository, and is made available under the terms and conditions applicable to Open Access Policy Articles, as set forth at <http://nrs.harvard.edu/urn-3:HUL.InstRepos:dash.current.terms-of-use#OAP>

## Share Your Story

The Harvard community has made this article openly available.  
Please share how this access benefits you. [Submit a story](#).

[Accessibility](#)

## **A macroscopic device described by a Boltzmann-like distribution**

Simon Tricard,<sup>#</sup> Claudiu A. Stan,<sup>#,\*</sup> Eugene I. Shakhnovich and George M. Whitesides<sup>\*</sup>

*Department of Chemistry and Chemical Biology, Harvard University, 12 Oxford Street,  
Cambridge, MA 02138*

---

<sup>\*</sup> corresponding authors: [claudiu.stan@alum.mit.edu](mailto:claudiu.stan@alum.mit.edu), [gwhitesides@gmwgroup.harvard.edu](mailto:gwhitesides@gmwgroup.harvard.edu)  
<sup>#</sup> these authors have contributed equally to this work

## **Abstract**

Equilibrium thermodynamic phenomena such as the Maxwell-Boltzmann distribution of molecular velocities are rare in systems of macroscopic particles interacting by mechanical collisions. This paper reports a system composed of millimeter-sized polymer objects that under mechanical agitation exhibits a “discretization” of the configurations of the system, and has a distribution of the probabilities of these configurations that is analogous to a Boltzmann distribution. The system is composed of spheres and a three-link chain on a bounded horizontal surface, shaken with an aperiodic but not completely random horizontal motion. Experiments were performed at different strengths of agitation (quantified by the frequency of agitation,  $f$ , at constant amplitude) and densities of spheres (quantified by the filling ratio, FR). The chain was typically found in one of three conformations—extended, single folded, and double folded—because, under collisions with the spheres, adjacent links were stable mechanically only when fully extended or fully folded. The probabilities of the different conformations of the chain could be described by a Boltzmann distribution in which the “temperature” depended on  $f$  and the “energies” of conformations on FR. The predictions of the Boltzmann formula using empirically determined “temperatures” and “energies” agreed with measurements within two experimental standard deviations in 47 out of 48 experiments.

## Introduction

A ubiquitous concept in statistical mechanics is the modeling of a gas by solid spherical particles colliding elastically in a box. This model is the first that most students encounter when they study statistical mechanics, and it explains clearly how thermodynamic properties (pressure, temperature, entropy, and many others) emerge as a result of molecular motions. The value of this model, aside from the validity of its analytical predictions, resides in its physically intuitive nature: it is built on basic concepts such as solid spherical particles and walls with precisely defined positions and velocities, perfectly elastic collisions, and so on.

It would be interesting to build a physical macroscopic model of a classical gas, even if only as a tool to teach statistical mechanics, but such a model is not (rigorously) possible because macroscopic systems are dissipative. In order to maintain motion in a macroscopic system, one needs to supply energy to the system, and driven systems are not in thermodynamic equilibrium. External driving is a technique often used in the field of granular physics, which studies mechanical ensembles of moving macroscopic particles whose intrinsic thermal motion is too small to be observed.<sup>1</sup> In most cases, mechanically agitated systems of macroscopic particles do not exhibit thermodynamic equilibrium properties, such as a Maxwell-Boltzmann distribution of particle velocities.<sup>2-3</sup>

It is nevertheless possible, though not trivial, to build physical systems of macroscopic particles whose motions mimic accurately the thermal agitation in a molecular gas. Examples of these systems are still rare,<sup>4-5</sup> and pose interesting questions: can characteristics of equilibrium thermodynamic behavior be observed in a dissipative driven system? Do non-equilibrium systems that obey the laws of thermodynamics exist—and why?

Here we report a model macroscopic system (made from polymer beads shaken on a horizontal flat surface) that we designed to mimic a fundamental statistical-mechanical problem: a system with discrete energy levels in thermodynamic equilibrium with a thermal bath. Our model system is made of three polymer cylinders joined by flexible links, immersed in an ensemble of free-rolling spheres, and shaken continuously. The first surprising behavior of the chain was an approximate “discretization”: though the links are continuously bendable, the chain was found most of the time in only three spatial conformations (extended, and folded in two different ways) to which we were able to assign distinct “energies”. The second surprising behavior was thermodynamic-like statistical behavior: the probability of the chain being in one of the conformations was approximately described by a Boltzmann-like distribution.

## **Background**

### **Physical-model simulations**

Physical-model simulations can be used to study systems whose behavior is too complex to be modeled based on analytical calculations. Physical models are less common than numerical simulations, because numerical simulations, which benefit from the constant improvements in computational power and the sophistication of software, are often less expensive. There are nevertheless cases in which the phenomena under study are too complicated to rely exclusively on computational simulations. Physical models are still being built to study environmental phenomena such as soil erosion<sup>6-7</sup>, atmospheric flows over rural terrains,<sup>8</sup> physiological systems and processes,<sup>9-10</sup> and technological procedures in metallurgy<sup>11-12</sup> and drilling.<sup>13</sup>

We are interested in physical-model simulations for a different reason: we want to build models that can be perceived with our senses (sight, primarily) of phenomena that can only be

observed with the aid of special tools, or for which direct component-level observations are not possible. We expect these physical models to guide our intuition about the phenomena that we simulate, and lead to discovery of new ones, because the human mind is specialized in interpreting information acquired by our senses.

As part of our previous explorations of self-assembly and of complexity, we have used ensembles of millimeter-sized objects to create several macroscopic models of molecular phenomena. The most ubiquitous phenomenon that we simulated was crystallization, which we could reproduce at the macroscopic scale using hard objects interacting by capillary<sup>14</sup> and electrostatic<sup>15-18</sup> forces. The capillary and electrostatic interaction potentials between objects were not identical to intermolecular potentials, but we could build a system with a particle interaction potential close in shape to intermolecular potentials, by using soft deformable objects that interacted by capillary forces; we used this system to simulate indentation fractures in crystals.<sup>19</sup> We also simulated the dynamic behavior of polymers using mechanically-agitated macroscopic beads arranged on a string, and we observed bending and folding phenomena in systems in which the beads either interacted via electrostatic forces<sup>20</sup> or did not.<sup>21</sup>

### **Granular matter as a physical model of molecular thermodynamic behavior**

Granular matter is composed of distinct particles; if the particles move independently from each other, a state that we will refer to as dynamic, the primary mechanism of interaction between particles is through collisions. Dynamic granular ensembles seem analogous to molecular gases, and attempts have been made to understand the properties of granular matter using the formalism of equilibrium thermodynamics.<sup>22</sup> Parameters such as the granular temperature<sup>23</sup> have been used as surrogates for the thermodynamic temperature and proved useful in understanding the

behavior of granular systems. The granular temperature  $T_G$  is equal to the average of the *fluctuations* of the kinetic energies of the particles. The velocity of the overall motion (the coarse-grained velocity of particles,  $\overline{v_c}$ ) must be subtracted from the velocity of particles,  $v$ , as shown in eqn (1), where  $m_G$  is the mass of the particles.

$$T_G = \frac{m_g}{2} \overline{(v - \overline{v_c})^2} \quad (1)$$

Granular matter in motion is a dissipative system, because collisions between particles are not elastic; external driving forces are required to maintain the movement of particles. The driving must be uniform, in the sense that all particles experience the same average driving force, to enable a thermodynamic distribution of the properties of particles; if the driving is not uniform, the granular temperature is highest near the driving source and decreases away from it.<sup>24-25</sup> Though necessary, uniform driving is not sufficient to create a physical model of a thermodynamic system at equilibrium. In two-dimensional, vertically-vibrated submonolayer experiments, the distribution of velocities of granular particles is not the Gaussian curve characteristic of a Maxwell-Boltzmann distribution.<sup>2-3</sup>

Experimental systems in which macroscopic objects behave similarly to molecules under thermal agitation have been reported previously.<sup>4-5</sup> The key to the success of these systems seems to be the randomization of the driving forces. In a first example, two layers of spheres, gravitationally-segregated because of their different densities, were agitated vertically by a bottom plate;<sup>4</sup> the two-dimensional velocities of particles from the top (but not the bottom) layer had a Gaussian distribution. In a second example, a granular mixture of spheres with two different sizes was sheared in a Couette cell (system thickness ~five monolayers, driven from both bounding surfaces); the diffusivity and the mobility of tracer particles embedded in this

system followed a Stokes-Einstein-type relation which was used to calculate the granular temperature.<sup>5</sup>

## **Experimental design**

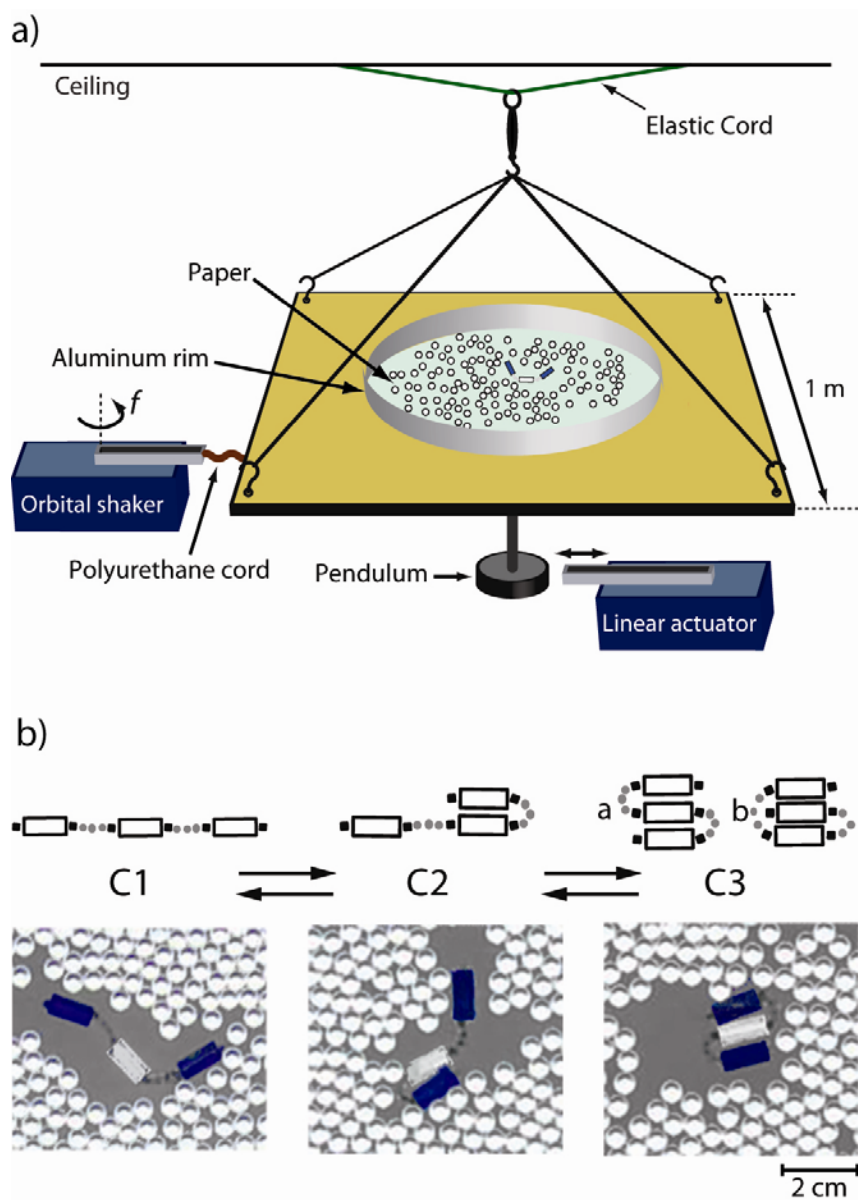
### **MecAgit: a horizontally-driven, two-dimensional granular system**

Our experimental system (Fig. 1(a)) consists of a flat horizontal surface on which we shake millimeter-sized objects within a region bounded by vertical walls. Compared to other horizontally shaken granular systems, ours is distinguished by its pseudo-random agitation motion,<sup>20</sup> which is a combination of orbital shaking with randomly timed “kicks”.

We prepared a circular mixing area with a diameter of 0.48 m using an aluminum rim, and we covered the area inside the rim with paper to generate an area with a constant friction coefficient on which the objects would roll, but not slide, when the plate was agitated. To avoid any possible electrical charging by contact electrification within the experimental setup, we maintained a relative humidity of more than 60% RH using a humidifier connected to the enclosed space above the plate.<sup>15</sup>



**Fig. 1** a) Experimental apparatus. Polymer spheres and a chain with flexible links are shaken with an aperiodic motion on a horizontal surface. b) The three observed conformations for the chain: extended (C1), partially folded (C2), and fully folded (C3).



In all experiments, we filled the mixing area with simple (spheres) and composite (cylinders connected by a string) polymeric objects, and shook them with a pseudo-random motion to simulate molecular phenomena. We will refer to this method of simulating molecular phenomena as “mechanical agitation”, or MecAgit.<sup>21</sup> The characteristics of MecAgit models are their two-dimensionality, the millimeter-size of the objects, the pseudo-random agitation, the possibility to design composite objects such as beads-on-a-string, and the control of long-range electrical interactions between objects by using different values of the relative humidity to suppress or allow contact electrification.

### **Designing a physical model of a canonical ensemble**

The canonical ensemble is one of the most useful statistic-mechanical concepts for predicting the thermal behavior of a system. The whole system is composed of a smaller system (therefore referred to as simply “system”) that has a range of possible states whose energy is known, and a thermal bath in which the system is immersed. If the states of the system have discrete energies, the probability  $P_i$  of the system being in a state with energy  $E_i$  depends exponentially on the absolute temperature  $T$ , and the probabilities are given by the Boltzmann distribution (eqn (2)), in which  $k_B$  is the Boltzmann constant, and the degeneracy  $g_i$  is the number of distinct states having the same energy  $E_i$ . The normalization factor is the partition function  $Z(T)$ , given by eqn (3), where the sum is conducted over all possible energies of the system.

$$P_i = \frac{1}{Z(T)} g_i e^{-\left(\frac{E_i}{k_B T}\right)} \quad (2)$$

$$Z(T) = \sum_i g_i e^{-\left(\frac{E_i}{k_B T}\right)} \quad (3)$$

To simulate a canonical ensemble using MecAgit, we needed a “thermal bath” and a “system”. The “thermal bath” was composed of free-rolling poly(methyl methacrylate) (PMMA) spheres with a diameter of 6.35 mm. We quantified the density of spheres in the system using the filling ratio (FR) parameter, defined as the ratio between the number of spheres in the system and the number of spheres required to fill completely the mixing area in a single layer with hexagonal packing.

The “system” (Fig. 1(b)) was a chain composed of three Nylon cylinders (6.35 mm diameter, 14 mm length) connected by flexible links (14 mm length) between cylinders. The chain could assume three folding conformations (Fig. 1(b)): (i) C1: unfolded, with none of the cylinders in contact and extended, (ii) C2: partially folded, with two cylinders in contact, and (iii) C3: fully folded, with all three cylinders folded together. There are two conformations C3, with the middle cylinder either at the center or at the periphery of the folded chain.

The experiments consisted of measurements of the probability of conformations as a function of  $f$  and FR. We recorded images of the system with a photo camera every 30 seconds for up to 30 minutes of continuous agitation, and we determined the type of conformation for each photograph using automated image analysis.

## **Results**

During agitation, the motion of the chain was caused by two driving forces: (i) friction with the agitating surface, and (ii) collisions with the PMMA spheres. Due to the design of our apparatus, the pseudo-random agitation engaged both the spheres and the chain, and was thus a uniform driving force. The mechanical driving of the chain was further randomized by collision with the spheres. The randomness of the overall driving of the chain and the dependence of conformation

probabilities on the frequency of agitation suggested that the statistics of the conformations of the chain would be analogous to the statistics of an equilibrium thermal system.

To demonstrate that the statistics of our system was analogous to a Boltzmann distribution, we used this reasoning: (i) we assumed first that the statistics of the system was described by a Boltzmann distribution (eqn (2)), (ii) we calculated the parameters of the Boltzmann distribution, *i.e.* the “energies” of the three conformations of the chain, and the “temperature” of the chain, for each experiment, and (iii) we concluded that the statistical behavior of the system was analogous to that of a canonical ensemble, because we could fit with good accuracy the probabilities of configurations using a small number of “energy” and “temperature” parameters.

### **The “discretization” of the shape of the chain during agitation**

We found that during agitation, the chain assumed the shape of one of the conformations C1, C2, or C3 in 93% of all photographs that we recorded. This “discretization” of shape to three distinct conformations during agitation was caused by the collisions with the spheres and by the particular relations between the sizes of the spheres, cylinders, and the mean free path of the spheres in our system. We can understand this phenomenon by considering a chain with two cylinders joined by a weakly elastic wire, colliding with an ensemble of spheres (with sizes comparable with those of cylinders) whose motion does not have a directional bias. If the angle between the two cylinders is  $180^\circ$  (*i.e.* an extended conformation), the two sides of a single cylinder are impacted (on average) at the same rate by spheres, and though the angle between cylinders might fluctuate, there is no net “sphere pressure”<sup>26</sup> to cause the folding of the chain. If, however, the angle between cylinders is less than  $180^\circ$  and the mean free path of spheres is

larger than the length of the cylinder, the sides of a cylinder that face the inside of the angle are partially shielded from sphere collisions by the other cylinder; in this case, there is a net “sphere pressure” that tends to reduce the angle and to fold the chain.

Depending on the stiffness of the link, there is a critical angle between the cylinders at which the tension of the link is balanced by the imbalance in sphere pressure. If the angle is larger than the critical angle, the elasticity of the link opens the chain; if the angle is smaller, the “sphere pressure” folds the chain. The two-cylinder chain is therefore a bistable system, with two stable equilibrium positions at cylinder angles of  $0^\circ$  and  $180^\circ$ , and one unstable equilibrium position at the critical angle. Our three-cylinder chain has three stable conformations; under the effect of fluctuations in the rate of collisions with spheres, the three-cylinder chain will be, for the majority of time, in one of its three conformations. The shape of the chain is thus “discretized”, in the approximate sense that only three conformations are *observed*.

The simple model we presented here to explain the predominance of C1, C2, and C3 conformations does not take into account biases in the motion of spheres, nor the fact that in our experiments, FR had values between 0.5 and 0.9, and the spheres therefore constituted a liquid-like rather than a gas-like system. We nevertheless believe that this model explains correctly the origin of “discretization” in our macroscopic system.

### **The dependence of the “energy levels” on the filling ratio**

Because the links between cylinders are elastic, the folded conformations C2 and C3 have a higher potential energy than the open conformation C1. The mechanical elastic energy stored in once (C2) or twice (C3) folded links is not identical to the “energies” of conformations C2 and C3 that are the parameters of a Boltzmann-like distribution. An important characteristic of our

system is that the statistic-mechanical “energies” associated with the three conformations of the chains depended on the filling fraction of the spheres. This dependence can be understood qualitatively using either of the two physical arguments below.

The mechanical energy needed to fold the chain when it is immersed in an ensemble of colliding spheres is less than the mechanical energy needed to fold the chain in the absence of collisions with spheres. When spheres are present, the chain needs to bend only as far as the critical angle for unstable equilibrium; past this point, the “sphere pressure” will complete the folding of the chain. At larger filling ratios, the surface density of spheres is larger, and thus the “sphere pressure” is larger; this fact brings the critical angle closer to  $180^\circ$  and reduces the energy needed for folding. As the filling ratio increases, the differences in “energy” between the three conformations are thus reduced, and, as we will show later, the “energies” of the three conformations can become approximately equal.

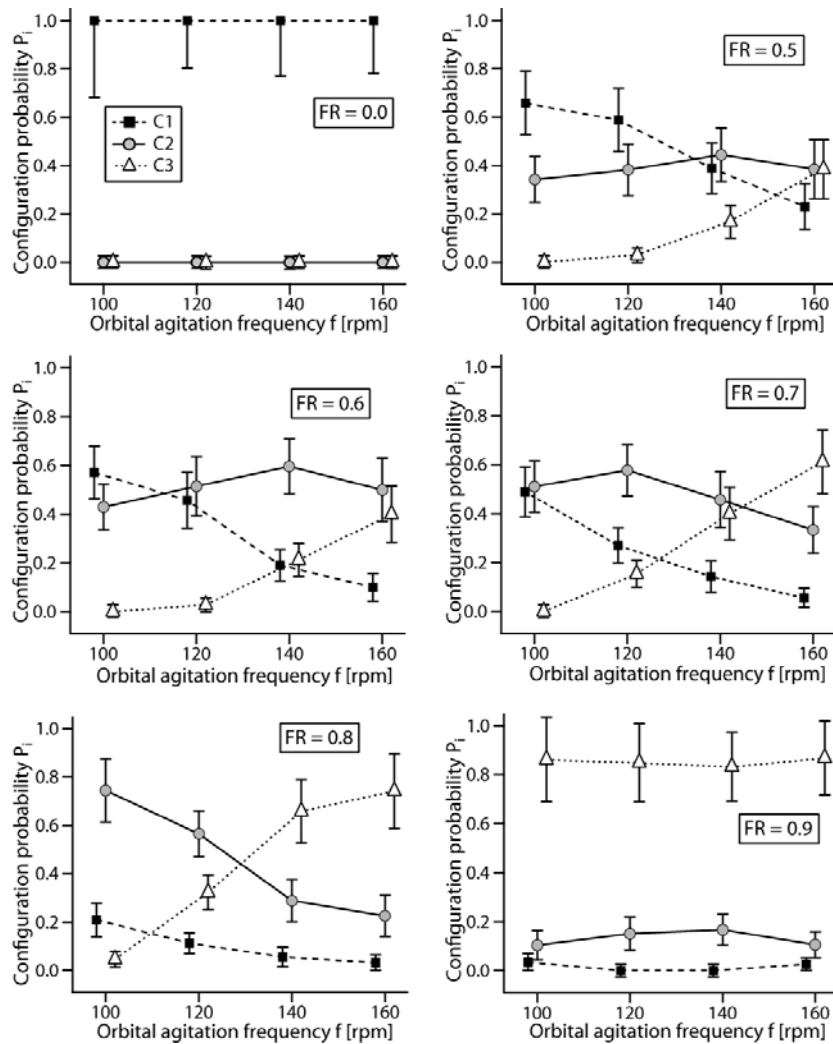
An alternate explanation of the dependence of folding energies on FR is based on the analogy between the three-cylinder chain and a polymer molecule. Flexible polymer molecules whose monomer units do not interact assume a coiled shape with an average end-to-end length that is smaller than the contour length of the polymer.<sup>25</sup> Coiling is a statistical phenomenon caused by thermal agitation (*i.e.*, collisions with solvent molecules), and leads to measurable entropic forces that compress stretched polymers to the coiled conformation.<sup>27-28</sup> In our system, sphere collisions tend to fold the three-cylinder chain, and the folding force is larger at higher filling ratios because the rate of collisions is larger. For the conditions of our experiments, these folding forces are “weaker” than the mechanical elasticity of the chain, and they reduce the *effective* stiffness of the chain, and thus the differences between the energies of the three conformations, by a degree that increases with the filling ratio.

### **The dependence of the conformation of the chain on FR and $f$**

Fig. 2 shows the probabilities  $P_i$  of all conformations  $C_i$  ( $i = 1, 2, 3$ ). We measured  $P_i$  for all combinations of FR values of 0.0, 0.5, 0.6, 0.7, 0.8, and 0.9, with  $f$  values of 100, 120, 140, and 160 rpm. Orbital agitation at frequencies below 80 rpm made spheres move collectively without any sphere-sphere collisions, corresponding to a granular temperature  $T_G = 0$ . At 80 rpm the spheres began to collide, but the evolution of the system towards a steady state was very slow. For orbital agitation frequencies above 160 rpm, the weight of the plate was not sufficient to maintain all four supporting cables extended, and the plate did not remain horizontal at all times. With the exception of the measurements at FR = 0.0 (no spheres), we chose the FR values to cover the widest range of filling fractions for which all three conformations were observed; for FR < 0.5, the chain either remained in the extended state, or the plate could not be leveled well enough to avoid movement of the chain towards the edge of the mixing area.

In the absence of spheres, the chain stayed extended (conformation C1) at all times, and  $P_1 = 1$  and  $P_2, P_3 = 0$ . From FR = 0.5 to FR = 0.8, as  $f$  was increased, conformation C1 (the lowest energy) became less probable, and conformation C3 (the highest energy) became more probable. A special case was encountered for a filling fraction of 0.9: within experimental uncertainty, the probabilities did not depend on  $f$  and  $P_1 < P_2 < P_3$ .

**Fig. 2** Probabilities,  $P_i$ , of the chain being in one of the conformations  $C_i$  (see Fig. 1(b)) as a function of the filling fraction  $FR$  and of the frequency of orbital shaker  $f$ . For filling fractions between 0.5 and 0.8, as  $f$  increases, the probability of the lowest-energy state  $C1$  decreases, and that of the highest-energy state  $C3$  increases, suggesting that  $f$  is related to the granular temperature of the system. The values of  $f$  were identical for all conformations; for clarity, data for  $C1$  and  $C3$  were shifted slightly along the x-axis. The error bars are the expected statistical errors, assuming a Poissonian distribution of the number of times,  $n_i$ , in which conformation was observed during an experiment (relative error:  $(n_i+1)^{-1/2}$ );  $n_i$  varied between 0 and 35 among all measurements.





## Calculation of the degeneracy of chain conformations

*Thermodynamic method.* We calculated the degeneracy values of the three conformations based on the number of folded shapes that cannot be transformed into each other by two-dimensional rotations and translations. A transition between two folded shapes of the same conformation can only happen if the chain assumes a different conformation during the transition. Fig. S1 in the ESI† shows all possible folded shapes: one for C1, two for C2, and four for C3. Identifying the number of folded shapes with the degeneracy values, we obtained  $g_1 : g_2 : g_3 = 1 : 2 : 4$ .

*Empirical method.* The assumption that allows the calculation of degeneracies based on symmetry arguments is that the system is composed of a large number of particles, and that it is at thermodynamic equilibrium. Our whole system has a relatively small numbers of particles and it is not in thermodynamic equilibrium. An alternative calculation of degeneracies is to evaluate them empirically using the property of the Boltzmann distribution (eqn (2)) that, if the energies of conformations are identical, the probabilities of conformations are independent of temperature and proportional to their degeneracies.

To identify the experimental conditions for which the three chain conformations had the same “energy”, we assumed that the “temperature” of the system is a function of the orbital agitation frequency  $f$ , because the kinetic energies of the objects increased as  $f$  increased. At FR = 0.9, the probabilities were approximately independent of  $f$  and thus independent of the “temperature”. Assuming that for FR = 0.9 the “energies” of configurations had the same value, we scaled the average probability of conformations to get the empirical degeneracy values  $g_1 : g_2 : g_3 = 1 : 9.5 : 60.5$ .

*The “optimal” degeneracy values.* The quality of the fit between the Boltzmann-like model and experimental results depended on the degeneracy values we used. Using the empirical

degeneracy numbers led to a much better agreement with the Boltzmann-like model than the thermodynamic degeneracy numbers. We also attempted to determine an optimal set of degeneracy numbers through numerical fitting, but we could not find one, because the fitting error function did not have a minimum at physically reasonable degeneracy numbers. We will report here only the Boltzmann-like parameters obtained using empirical degeneracies.

### **Modeling the statistics of chain conformations with a Boltzmann distribution**

The dependence of the probabilities of conformations on  $f$  for filling ratios from 0.5 to 0.8 (Fig. 2) is similar to the dependence of the populations of a system with three energy levels on temperature. This similarity suggested that the probability of C1, C2 and C3 conformations might be described mathematically by a Boltzmann distribution (eqn (2)) in which the energies  $E_i$  and the temperature  $T$  are functions of the experimental parameters  $f$  and FR.

Mathematical fitting of the probabilities of configurations could lead to macroscopic parameters for  $E_i$  and  $T$  that are complicated functions of  $f$  and FR, but intuitively, the “temperature” should be related to the frequency of agitation, and the “energy levels” on the rate of the impacts of spheres on the chain, which is in turn related to the density of spheres, quantified by the filling ratio. With the assumption that the “temperature” depends on  $f$  but not on FR, and the “energies” depend on FR but not on  $f$ , the Boltzmann-like equation for probabilities of conformations becomes:

$$P_i(f, FR) = \frac{1}{Z(f, FR)} g_i e^{-\left(\frac{E_{i,MA}(FR)}{T_{MA}(f)}\right)}, \quad i = 1, 2, 3 \quad (4)$$

In eqn (4) we defined the “MecAgit temperature”  $T_{MA}$ , and the “MecAgit energies”  $E_{i,MA}$ , which are measured in the same energy units (*e.g.* Joules). This definition is equivalent to

choosing the “Boltzmann-like constant”  $k_{B, MA} = 1$  in the Boltzmann-like equation; therefore, eqn (4) does not contain a “Boltzmann-like constant”.

The fitting of measured probabilities to eqn (4) is difficult because of its nonlinearity. Instead, in order to determine  $E_{i,MA}(FR)$  and  $T_{MA}(f)$ , we first linearized eqn (4) by eliminating the partition function  $Z(f, FR)$ . Eqn (5) shows that the ratio of populations of two conformations does not depend on  $Z$ :

$$\frac{P_j}{P_1} = \frac{g_j}{g_1} e^{-\left(\frac{E_{j,MA} - E_{1,MA}}{T_{MA}}\right)}, j = 2, 3 \quad (5)$$

Because only the differences between energy levels are relevant in our analysis, we adopted the convention that  $E_{1,MA} = 0$ . With this convention, we used eqn (6) to calculate the values of  $E_{2,MA}/T_{MA}$  and  $E_{3,MA}/T_{MA}$  from the conformation probabilities  $P_i$  (see Fig. S2 in the ESI†). Using these values, we calculated  $T_{MA}$  as a function of  $f$  by averaging the data from experiments performed at different FR values, using eqn (7).

$$\frac{E_{j,MA}}{T_{MA}} = -\ln\left(\frac{P_j}{P_1} \frac{g_1}{g_j}\right), j = 2, 3 \quad (6)$$

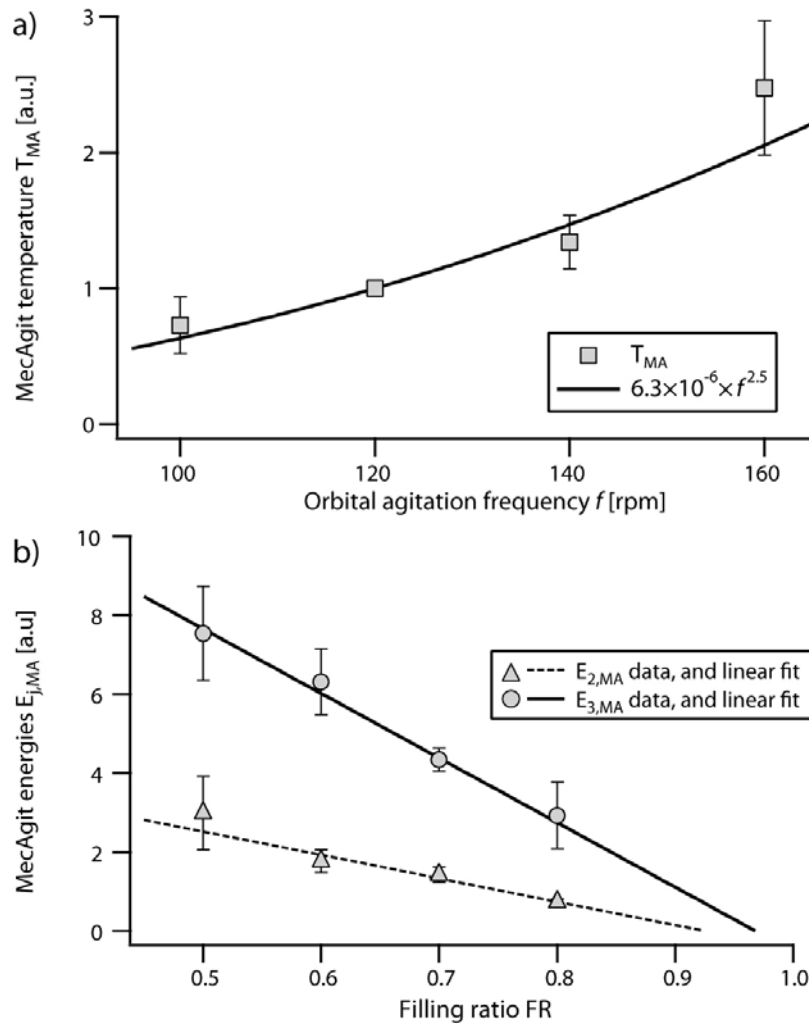
$$T_{MA}(f) = \frac{1}{n_{j,FR}} \sum_{j,FR} T_{MA}(120) \times \frac{E_{j,MA}/T_{MA}(120, FR)}{E_{j,MA}/T_{MA}(f, FR)} \quad (7)$$

In eqn (7),  $n_{j,FR}$  is the number of non-zero  $P_2$  and  $P_3$  probabilities measured at the same  $f$  but different FR values ( $n_{j,FR} = 7$  or  $8$  depending on  $P_3$ ; we did not use experiments for which  $P_3 = 0$  because they made  $E_{3,MA}/T_{MA}$  infinite). We defined the units of temperature such that  $T_{MA} = 1$  at  $f = 120$  rpm.<sup>29</sup> Fig. 3(a) shows the dependence of  $T_{MA}$  values as a function of agitation frequency, which could be fitted with good accuracy to a power-law dependence:  $T_{MA} = 6.3 \times 10^{-6} \times f^{2.5}$ .

We calculated the energies  $E_{2,MA}$  and  $E_{3,MA}$  of the C2 and C3 conformations according to eqn (8), where  $n_f$  is the number of non-zero probability measurements carried at a given frequency  $f$  ( $n_f = 3$  or  $4$ ). The dependence of the energy levels on FR, shown in Fig. 3(b), was approximately linear, and the linear dependence extrapolated to zero at  $FR = 0.95 \pm 0.03$ , in approximate agreement with our earlier assumption that the energy levels were degenerate at  $FR = 0.9$ .

$$E_{j,MA}(FR) = \frac{1}{n_f} \sum_f \frac{E_{j,MA}(f, FR)}{T_{MA}(f)} \times T_{MA}(f) \quad (8)$$

**Fig. 3** The MecAgit temperature and energies  $T_{MA}$  and  $E_{j,MA}$ . (a) The values of TMA as a function the frequency of agitation  $f$ , calculated after choosing  $T_{MA} = 1$  at 120 rpm. The symbols represent the  $T_{MA}$  data, and the line shows the best power-law fit of the data,  $T_{MA} \sim f^{2.5}$ . (b) The configuration energies  $E_{2,MA}$  and  $E_{3,MA}$  as a function of the filling ratio FR. The symbols represent the measurements, and the lines are linear fits weighted by the standard error of measurements. The error bars in all graphs represent one standard deviation of the measurements (seven or eight measurements for  $T_{MA}$ ; three or four measurements for  $E_{j,MA}$ ).

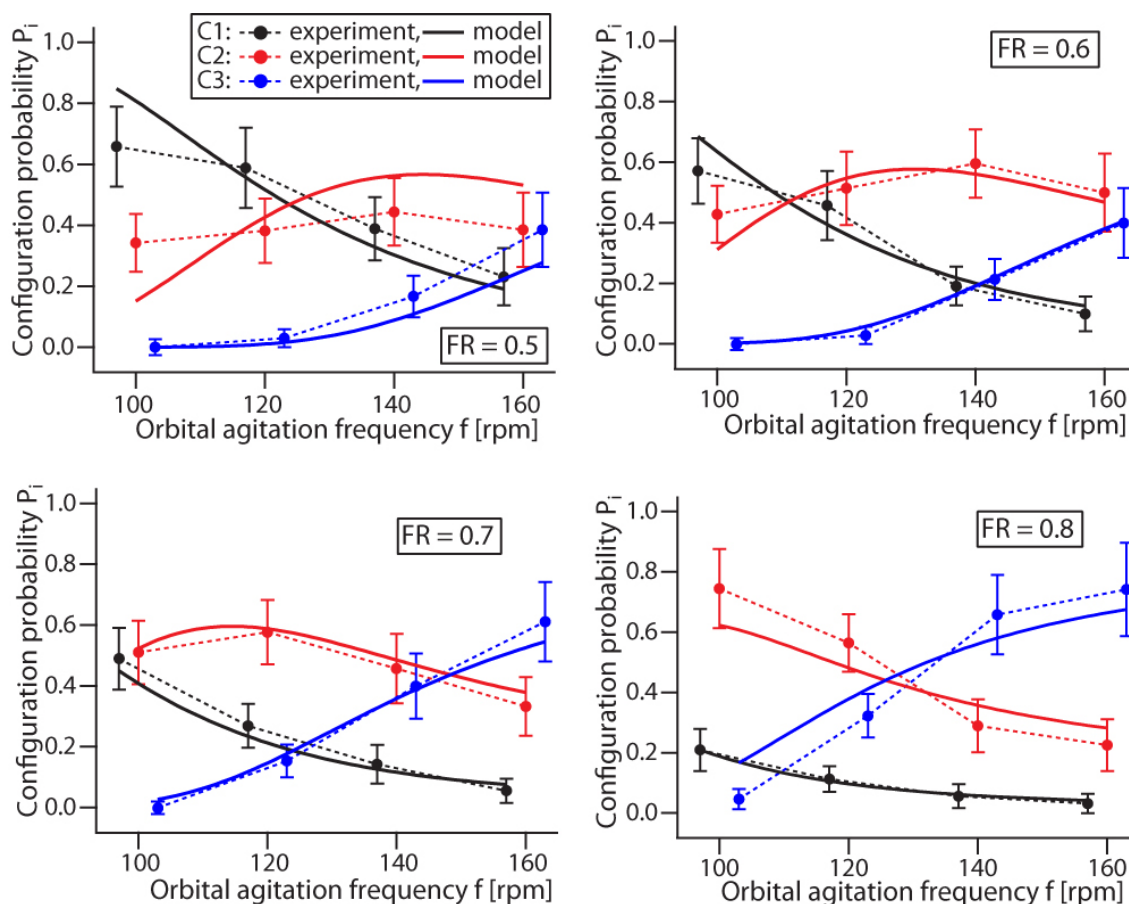


To verify the validity of our analogy between our system and a canonical ensemble, we calculated the probabilities of conformations using the Boltzmann-like distribution (eqn (4)) with the fitted functions shown in Fig. 3 (power-law in  $f$  for  $T_{MA}$ , and linear in FR for  $E_{j,MA}$ ), and compared them with experimental measurements. Fig. 4 shows that the Boltzmann-like statistics provided a good description of the behavior of the system; 38 of the 48 calculated probabilities fell within one standard deviation of measured probabilities, and 47 of 48 fell within two standard deviations. Overall, the Boltzmann-like statistics were most accurate at  $FR \geq 0.6$  and  $f \geq 120$  rpm; experiments at  $FR = 0.5$  were close to the regime in which the chain stayed always extended, and experiments at  $f = 100$  rpm were close to the regime in which all spheres moved together.

## Discussion

Among the macroscopic parameters in the Boltzmann-like model, the MecAgit temperature has the clearest relation to the microscopic temperature, qualitatively and quantitatively. The power-law proportionality between  $T_{MA}$  and  $f^{2.5}$  reflects the concept that the temperature is a measure of kinetic energy, because the velocity of the shaking table is proportional to  $f$ . The significance of the energy levels  $E_{i,MA}$  and of the degeneracy numbers  $g_i$  are also qualitatively clear: the energy levels arise due the mechanical bistability of the conformation of adjacent links in the chain (*i.e.*, either folded or extended) under random collisions with the spheres, and the degeneracy numbers reflect the fact that there are more possible paths to the folding of a given configuration than to its unfolding.

**Fig. 4** Comparison between experimental measurements and the predictions of the Boltzmann-like statistics with experimentally determined “energies” and “temperatures”, for frequency ratios  $0.5 \leq FR \leq 0.8$ . The symbols connected by thin dashed lines are the experimental measurements (also shown in Fig. 2), and the thick solid lines the predictions of the Boltzmann-like statistics. For clarity, the data sets for the C1 and C3 conformations have been shifted horizontally, slightly, from the measurement values, which are shown on the x-axis.



The MecAgit energy levels  $E_{j,MA}$  in our system are different from those of atomic systems because they depend strongly on FR, while the electronic levels of atoms, molecules, and crystals depend only weakly on pressure at ambient conditions; relative changes in the electronic energy levels comparable to those observed in our MecAgit system are possible, but they require pressures thousands of times larger than atmospheric pressure.<sup>30</sup>

The Boltzmann-like statistics provided a significantly better fit with the measurements when they included the empirical degeneracy values. For comparison, Fig. S3 in the ESI† shows the predictions of the Boltzmann model based on thermodynamic degeneracies, in the same format used in Fig. 4 for the case of empirical degeneracies. We could not find a way to calculate a set of degeneracy values that would agree with the empirical degeneracies, but we believe that such a calculation would be dependent on the details of the system. The relative size of the chain and the spheres or the surface density of spheres might suppress some of the folding or unfolding mechanisms, which are analogous to the “reaction paths”<sup>31</sup> in the transitions between reagents and products in a chemical reaction.

## **Conclusion**

We have developed a new granular system, composed by a chain surrounded by free spheres in a two-dimensional configuration, which exhibited a phenomenon analogous to a microscopic system with discrete energy levels: the distribution of the probabilities of the different configurations of the system was mathematically analogous to a Boltzmann distribution. Our system exhibited a behavior characteristic to non-dissipative systems, although it was dissipative due to mechanical friction and inelastic collisions. We believe that the unusual thermodynamic-analogous behavior in our driven granular system is due to the uniform driving of all objects by



the shaking surface, and due to the randomization of the motion of the chain. Randomization of the motion of the chain in our system was achieved by a combination of the aperiodic movement of the shaking surface with collisions between the chain and independently-moving spheres.

The system presented here is a first attempt to create a granular system which is analogous to a thermodynamic system with discrete energy levels, and it provides a new parameter for the “temperature” of a granular system—the MecAgit temperature  $T_{MA}$ . A comparison between  $T_{MA}$  and the granular temperature  $T_G$  characteristic to the spheres would be useful in determining the applicability and advantages of using  $T_{MA}$  and  $T_G$  as surrogates for the thermodynamic temperature; for this study we could not measure the sphere velocities which are required to calculate  $T_G$ , because we recorded only static images of the system.

The system and the results reported here are part of a larger program in which we aim to physically model microscopic phenomena at the macroscopic scale. One of the goals of this program is to build systems that enhance our intuition of microscopic phenomena, but such systems could be useful outside the lab as well. The MecAgit system is simple and inexpensive enough for implementation in classroom teaching, where physical models have been shown to engage students and increase their level of understanding.<sup>32-33</sup>

## **Acknowledgments**

We thank Dr Phillip W. Snyder, Dr Antoine Venaille, and Dr Meital Reches for insightful discussions, and Dr Elizabeth Maxwell for editing advice. This work was primarily supported by the US Department of Energy, Division of Materials Sciences & Engineering, under Award No. DE-FG02-OOER45852. GMW acknowledges salary support from the US Department of Energy, Office of Basic Energy Sciences, under Award No. DE-SC0000989.

## Notes and references

\* *Department of Chemistry and Chemical Biology, Harvard University, 12 Oxford Street, Cambridge, MA 02138. E-mail: claudiu.stan@alum.mit.edu, gwhitesides@gmwgroup.harvard.edu*

# These authors have contributed equally to this work.

† Electronic Supplementary Information (ESI) available, containing: (1) additional information about the experimental setup; (2) all distinct folding shapes for each conformation of the chain; (3) values of the  $E_{j,MA}/T_{MA}$  parameters for distinct experiments; and (4) a comparison between experimental measurements and the predictions of the Boltzmann model based on thermodynamic degeneracy values. See DOI: 10.1039/b000000x/

1. I. S. Aranson and L. S. Tsimring, *Rev. Mod. Phys.*, 2006, **78**, 641-692.
2. J. S. Olafsen and J. S. Urbach, *Phys. Rev. Lett.*, 1998, **81**, 4369-4372.
3. J. S. Olafsen and J. S. Urbach, *Phys. Rev. E*, 1999, **60**, R2468-R2471.
4. G. W. Baxter and J. S. Olafsen, *Nature*, 2003, **425**, 680-680.
5. C. M. Song, P. Wang and H. A. Makse, *P. Natl. Acad. Sci. USA*, 2005, **102**, 2299-2304.
6. E. Védie, J. L. Lagarde and M. Font, *Earth Surf. Proc. Land.*, 2011, **36**, 395-407.
7. V. Bagarello and V. Ferro, *Catena*, 2012, **95**, 1-5.
8. H. Kozmar, *Environ. Fluid Mech.*, 2012, **12**, 209-225.
9. I. R. Titze, S. S. Schmidt and M. R. Titze, *J. Acoust. Soc. Am.*, 1995, **97**, 3080-3084.
10. I. Jurjevic, M. Rados, J. Oreskovic, R. Prijic, A. Tvrdeic and M. Klarica, *Collegium Antropol.*, 2011, **35**, 51-56.
11. B. Wright, P. Zulli, Z. Y. Zhou and A. B. Yu, *Powder Technol.*, 2011, **208**, 86-97.
12. D. G. Ma, W. Q. Chen and X. M. Che, *Can. Metall. Quart.*, 2012, **51**, 31-38.
13. C. C. Hird, Q. Ni and I. Guymmer, *Geotechnique*, 2011, **61**, 993-999.
14. N. B. Bowden, M. Weck, I. S. Choi and G. M. Whitesides, *Accounts Chem. Res.*, 2001, **34**, 231-238.

15. B. A. Grzybowski, A. Winkleman, J. A. Wiles, Y. Brumer and G. M. Whitesides, *Nat. Mater.*, 2003, **2**, 241-245.
16. G. K. Kaufman, M. Reches, S. W. Thomas, J. Feng, B. F. Shaw and G. M. Whitesides, *Appl. Phys. Lett.*, 2009, **94**, 044102.
17. G. K. Kaufman, S. W. Thomas, M. Reches, B. F. Shaw, J. Feng and G. M. Whitesides, *Soft Matter*, 2009, **5**, 1188-1191.
18. R. Cademartiri, C. A. Stan, V. M. Tran, E. Wu, L. Friar, D. Vulis, L. W. Clark, S. Tricard and G. M. Whitesides, *Soft Matter*, 2012, **8**, 9771–9791.
19. V. R. Thalladi, A. Schwartz, J. N. Phend, J. W. Hutchinson and G. M. Whitesides, *J. Am. Chem. Soc.*, 2002, **124**, 9912-9917.
20. M. Reches, P. W. Snyder and G. M. Whitesides, *P. Natl. Acad. Sci. USA*, 2009, **106**, 17644-17649.
21. S. Tricard, E. Feinstein, R. F. Shepherd, M. Reches, P. W. Snyder, D. C. Bandarage, M. Prentiss and G. M. Whitesides, *Phys. Chem. Chem. Phys.*, 2012, **14**, 9041-9046.
22. I. S. Aranson and L. S. Tsimring, *Granular patterns*, Oxford University Press, Oxford, 2009.
23. P. K. Haff, *J. Fluid Mech.*, 1983, **134**, 401-430.
24. A. Kudrolli, M. Wolpert and J. P. Gollub, *Phys. Rev. Lett.*, 1997, **78**, 1383-1386.
25. E. L. Grossman, T. Zhou and E. BenNaim, *Phys. Rev. E*, 1997, **55**, 4200-4206.
26. S. Aumaitre, C. A. Kruelle and I. Rehberg, *Phys. Rev. E*, 2001, **64**, 041305.
27. M. D. Wang, H. Yin, R. Landick, J. Gelles and S. M. Block, *Biophys. J.*, 1997, **72**, 1335-1346.
28. C. G. Baumann, S. B. Smith, V. A. Bloomfield and C. Bustamante, *P. Natl. Acad. Sci. USA*, 1997, **94**, 6185-6190.
29. We chose  $f = 120$  rpm for reference because it was the lowest agitation frequency for which we observed all three conformations at filling fractions ranging from 0.50 to 0.80.
30. J. M. Besson, W. Paul and A. R. Calawa, *Phys. Rev.*, 1968, **173**, 699-713.
31. D. M. Bishop and K. J. Laidler, *J. Chem. Phys.*, 1965, **42**, 1688-1691.
32. A. M. Ingham and J. K. Gilbert, *Int. J. Sci. Educ.*, 1991, **13**, 193-202.
33. A. E. Rivet and K. A. Kastens, *J. Res. Sci. Teach.*, 2012, **49**, 713-743.